Zero Gap Alkaline Electrolysis Cell Designs for Renewable Energy Storage as Hydrogen Gas

Robert Phillips,[a] and Charles W. Dunnill.[a]*

Zero gap alkaline electrolysers hold the key to cheap and efficient renewable energy storage via the production and distribution of hydrogen gas. A zero gap design, where porous electrodes are spacially separated only by the gas separator, allows the unique benefits of alkaline electrolysis to be combined with the high efficiencies currently only associated with the more expensive PEM set-up. This review covers the basics of alkaline electrolysis, and provides a detailed description of the advantages of employing a zero gap cell design over the traditional arrangement. A comparison of different types of zero gap cell designs currently seen in research is made, and a description of recent developments is presented. Finally, the current state of research into zero gap alkaline electrolysis is discussed, and pathways for future research identified. Zero gap alkaline electrolysis will allow excess renewable energy to be stored, transported and used on demand in a green and environmentally friendly manner as when the hydrogen is burnt or passed into a fuel cell it produces only water and energy.

1. Introduction

The electrolysis of water has been known for over 200 years, and is achieved by applying a voltage across two electrodes in water, splitting the water molecules into its constituent elements of two parts hydrogen and one part oxygen. The hydrogen can be stored as a green fuel as when recombined with the oxygen yields energy and only water as the by-product. Pure water is, however, known to be a poor conductor of electricity and therefore inefficient for electrolysis.[1] Water soluble electrolytes are added to improve conductivity and hence the efficiency of the process. Electrolysis can be performed under acidic, neutral or basic conditions depending on the electrolyte used. Acidic conditions lead to severe corrosion of common metals, and thus require the use of expensive precious metals as electrodes, resulting in high capital costs. Neutral electrolysis using sodium chloride is energetically expensive, and results in environmentally questionable side reactions such as the production of hydroxide and chlorine gas. Alkaline conditions allow for the use of cheaper earth abundant metals as electrodes, but generally operate at a lower efficiency, requiring larger devices and thus higher costs. Highly efficient alkaline electrolysis could hold the key to cheap and efficient water splitting.

Electrolysis of water is of key concern to modern life as it holds the potential to store large quantities of renewable energy in the form of hydrogen gas. Hydrogen can be used as a universal energy carrier to deliver renewable energy around a network whist simultaneously buffering supply and demand. At the point of use hydrogen is recombined with oxygen to form only water and yield its stored energy, completing the carbon free cycle. This is critical to the modern energy infrastructure as we turn towards a more diverse renewable energy dominated landscape. The transition to such a landscape will inevitably consist of a change from a "one to many" distribution network, traditionally seen as a central power station delivering power to a grid of houses, into a "many to many" network where multiple sources of energy such as solar panels on houses feed into the network from multiple locations. A universal, time independent energy carrier such as hydrogen is therefore imperative to balance the network.

Traditional alkaline electrolysis based on two electrode plates separated by a liquid alkaline electrolyte suffers from low current densities (<0.25 $A \cdot cm^{-2}$) with efficiencies typically only in the region of up to <60 %.[2-4] These relatively low efficiencies encouraged the development of other water splitting technologies, most notably the acidic Proton Exchange Membrane (PEM) Electrolysis and more recently Solid Oxide Electrolysis.[5, 6] PEM cells operating at around 2 $A \cdot cm^{-2}$ and 1.7 V giving 72 % efficiency have been developed,[5, 7] although the benefits of this high performance is offset by the high costs of both the Nafion membrane, and the noble catalysts such as platinum and iridium necessary due to the acidic environment. Solid oxide electrolysis requires significantly high operating temperatures, adding additional energy inputs. PEM electrolysers work using a proton exchange membrane as the electrolyte, and employing a zero gap cell design where the electrodes are deposited directly onto the membrane.[5]

The alkaline environment offers the significant advantage of using cheap and abundant metals for catalysts and other cell components, whereas PEM offers high performing electrolysis cells at the expense of capital cost. Combining the benefits of both alkaline and PEM electrolysis, electrolysers running at high current densities and efficiencies can be developed at low cost.[8] An important step towards these 'Advanced Alkaline Electrolysers' is employing a cell design based around the zero gap concept.

In alkaline electrolysis, the zero gap cell design works by compressing two porous electrodes either side of a hydroxide ion conducting membrane or gas separator.[9] This achieves a gap between the two electrodes equal to the thickness of the membrane (<0.5 mm) rather than (>2 mm) for the traditional setup, thus significantly reducing the Ohmic resistance contribution from the electrolyte between the two electrodes. A gas diffusion layer provides an electrical connection from the porous electrode to the bipolar plate, whilst simultaneously

allowing a feed of electrolytic solution, and the removal of the gas products.

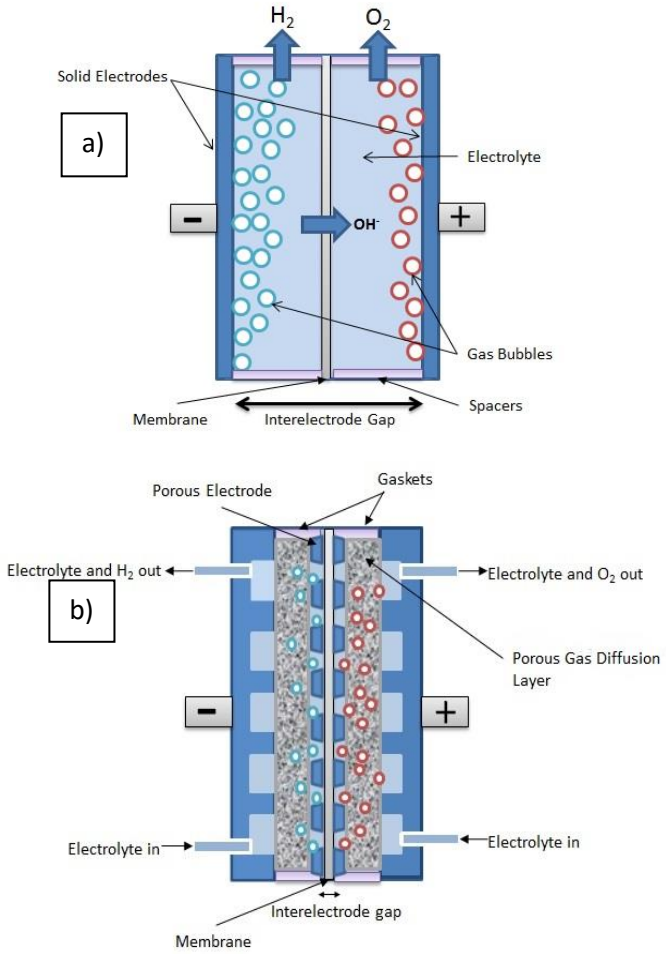

Figure 1. a) Standard Setup, b) Zero Gap Setup - showing the principal differences in design, porous electrodes are pressed either side of the gas separator to reduce the inter-electrode gap, and a conducting gas diffusion layer provides an electrical connecting from the electrodes to the bipolar current collector.

Figure 1 shows that the main difference between the traditional setup and the zero gap design is the employment of porous electrodes rather than solid metal plates. This allows cells with a very small inter-electrode gap, compact design and high efficiency. It forces gas bubbles to be released from the backside of the electrodes, reducing their contribution to the cell voltage.[10]

Zero gap alkaline electrolysis was first proposed in 1967 by Costa and Grimes, using mesh electrodes either side of a microporous gas separator.[11] Significant research was undertaken during the 1980's showing a large increase in current density.[12] Recent research has been principally centred on the development of Alkaline Anion Exchange Membranes,[13, 14] which offer advantages of lower resistance and improved gas separation properties over the previously used microporous gas separators. Novel cell designs have also been developed including the use of high surface area foam electrodes, and adopting fuel cell type electrodes deposited directly onto the membrane.

2. Basics of Alkaline Electrolysis

2.1 Cell Potential of Water Electrolysis Cell

The basic process of electrolysis is the splitting of water into its two elemental components (Hydrogen and Oxygen) according to the following:

$$2H_2O_{(l)} \rightarrow 2H_{2(g)} + O_{2(g)}$$

This is achieved by applying DC potential across two electrodes immersed in a liquid electrolyte.

For alkaline electrolysis, a strong base, is used as the electrolyte to reduce the resistance of the solution. Under standard conditions, and a pH of 14, the half-cell reactions are as follows:

Cathode: $2H_2O + 2e^- \rightarrow H_2 + 2OH^-$
$(E^0 = -0.83\ V\ vs.SHE\ at\ pH\ 14)$

Anode: $2\mathrm{OH}^- \rightarrow \mathrm{H_2O} + \frac{1}{2}\mathrm{O_2} + 2\mathrm{e}^-$
$(E^0 = 0.40\ V\ vs.SHE\ at\ pH\ 14)$

The total reversible cell voltage (E_{Rev}) is calculated using the cell potentials of the two half-reactions. Following normal convention, the half reactions are considered to be an oxidation and reduction respectively:[2]

$$E_{Rev} = E_{Anode} - E_{Cathode}$$

It can therefore be shown that for standard conditions, E_{Rev} = 1.23 V. The E^0 values at the anode and cathode are pH dependant however the E_{Rev} of 1.23 V is maintained. In practice this is never achieved as there is an overpotential that must be applied to drive the theoretical process.

2.2 Actual Cell Voltage

The actual cell voltage is distinct from the reversible cell voltage due to inefficiencies in the system, the actual cell voltage can be broken down into its contributing factors:

$$E_{Cell} = E_{Rev} + \eta_{Anode} + \eta_{Cathode} + I \times R_{Cell}$$

Where η_{Anode} is the overpotential at the anode, $\eta_{Cathode}$ the overpotential at the cathode, I the current and R_{Cell} the cell resistance.

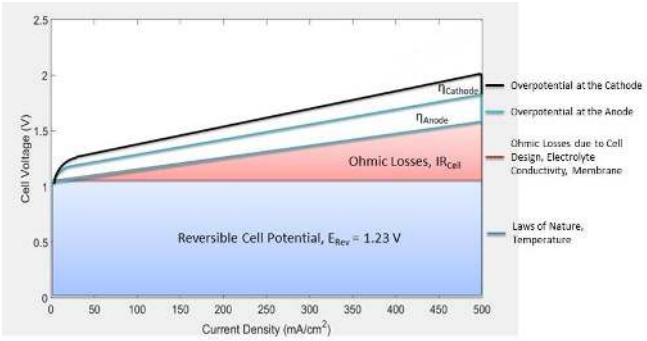

Figure 2. – Graph showing the individual contributions to cell voltage, this allows each contribution to be targeted individually, allowing a systematic approach to reducing the cell voltage. [15, 16]

Figure 2 shows how the magnitude of the contributions to cell voltage vary with current density. With increasing current densities the contribution from Ohmic losses becomes more prominent, becoming the dominant factor at high values. The overpotential at the anode can be seen to be greater than that at the cathode.

2.3 Cell Efficiency

The efficiency of an electrolysis cell can be defined as the ratio of useful energy output to the total energy input.

$$Efficiency = \frac{Useful\ Energy\ Output}{Total\ Energy\ Input} =$$

$$\frac{Energy\ content\ of\ 1\ mole\ of\ hydrogen}{Energy\ required\ to\ produce\ 1\ mole} = \frac{283.8\ (kj)}{E_{cell} it}$$

Where 283.8 kj is the high heating value of one mole of hydrogen, and is the time taken for one mole of hydrogen to be produced.

An alternative description for the efficiency can be made using the relation between the ideal and actual cell voltages (at standard conditions):

$$\frac{E_{Rev} \times I \times t}{E_{Cell} \times I \times t} = \frac{E_{Rev}}{E_{Cell}} = \frac{1.23\ V}{E_{Cell}}$$

Research has been focused on increasing cell efficiency, which can be achieved by reducing contributions to the cell voltage from the electrode overpotentials and the cell resistance. This review focuses on the cell resistance, which is independent of electrocatalyst material, and can be broken down further:

$$R_{Cell} = R_{Circuit} + R_{Electrolyte} + R_{Bubbles} + R_{Membrane}$$

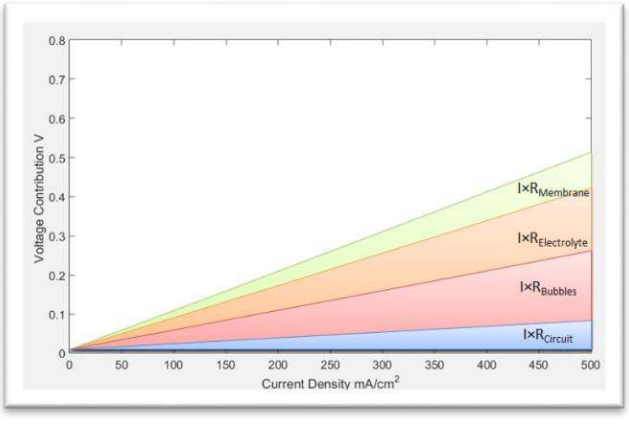

Figure 3. – Graph showing the contributions to cell voltage from the components of the cell resistance. These contributions can be targeted individually to reduce the overall cell resistance.

Figure 3 represents the contributions to the cell voltage from the components of the cell resistance. Research is focused on reducing the overall contribution by targeting individual contributions, bringing the cell performance towards the theroretical optimum even under high curent density operation.

3. Advantages of the Zero Gap Design

The zero gap design facilitates the reduction of the cell resistance contributions from both the electrolyte and gas bubbles, $R_{Electrolyte}$ and $R_{Bubbles}$.

3.1 Resistance due to Electrolyte $R_{Electrolyte}$

The voltage drop due to the electrolytic solution is expressed using Ohms law:

$$IR_{Electrolyte} = \frac{Il}{A\kappa} = \frac{il}{\kappa}$$

Where I is the current in amperes (A), i is the current density in A·cm^{-2}, l is electrode spacing in cm, A is the cross-sectional area in cm^2, and κ is the conductivity in Siemens per cm (S·cm^{-1}).

Ohms law implies that in order to reduce voltage drop at the same current density, either conductivity (κ) needs to be increased, or the electrode spacing (l) needs to be decreased. Conductivity has been optimised in previous studies for the most commonly used electrolytes; Potassium Hydroxide (KOH) and Sodium Hydroxide (NaOH).[17] Therefore reducing the distance between the electrodes is crucial to reduce the resistance contributions from the electrolyte. There is also a health and safety aspect to be considered when using high concentrations of the alkaline electrolyte, as the caustic solution can pose a serious risk to operators.[3]

Using the traditional setup, Nagai *et al.*[18] found that at current densities above 0.5 A·cm^{-2}, the optimal gap between electrodes was greater than 2 mm, due to the contribution to cell resistance from the gas bubbles produced.

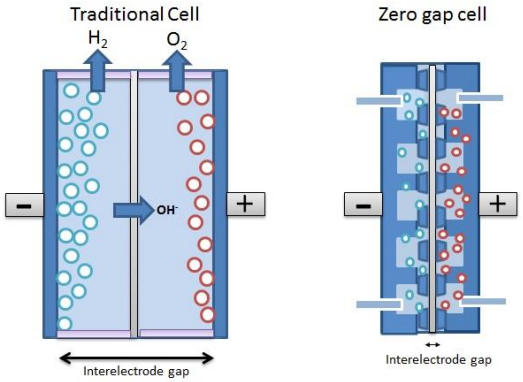

Figure 2 – Schematic showing reduction of inter-electrode gap from employing a zero gap cell design. This significantly reduces the overall cell resistance, increasing performance, particularly at high current densities. Note the loss in direct surface area between the pates due to the bubbles in the conventional design.

The zero gap design, *figure 4,* allows the inter-electrode gap to be as small as the thickness of the membrane or gas separator used, i.e. less than 0.5 mm, and with future membrane improvements this distance will be reduced further.

3.2 Bubble Resistance ($R_{Bubbles}$)

The generation of gas bubbles introduces two sources of inefficiencies into the system; firstly due to the coverage of the electrode during the growth of the gas bubble, and secondly once the gas bubble has been released from the surface of the electrode, as shown in *figure 4*.

3.2.1 Electrode Coverage

The current actually flows through a smaller surface area than the geometric surface area of the electrode as a result of the bubble coverage,[19] increasing the actual current density compared to the nominal current density. It is the actual current density that controls the overpotential, as well as controlling the contribution to the Ohmic drop across the double layer adjacent to the electrode.

The actual current density, j, can be expressed in terms of the superficial current density, I, and the fraction of a gas-evolving electrode surface covered by adhering bubbles, θ :[20]

$$j = \frac{I}{1-\theta}$$

It can be seen that the actual and superficial current densities are equal when the bubble coverage θ is zero, which is impossible as whenever current flows, there is by definition bubble growth.

Experimental data collated by Nagai *et al.* suggested an approximate relationship between superficial current density and bubble coverage could be made as: $\theta = 0.365(j)^{0.3}$, although it is noted that other parameters also affect the bubble coverage. *Figure 5* shows that superficial current densities above 0.1 A·cm^{-2}), show large fractional coverage, in the region of 0.3.[20]

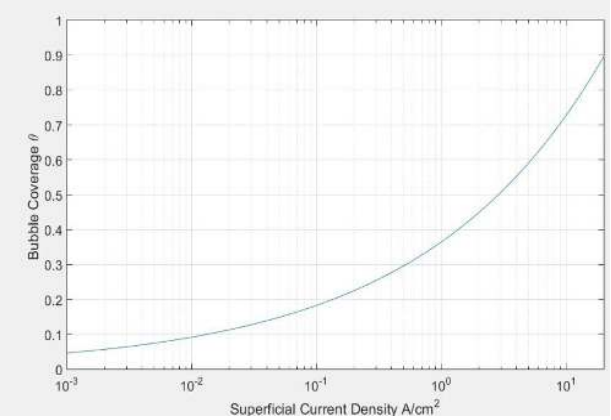

Figure 3 - Relationship between superficial current density and bubble coverage, based on experimental data,(Vogt *et al*[19]) at current densities above 1Acm^{-2}, the bobble coverage becomes substantial, reducing the available electrode area.

The increased contributions to the cell voltage from the overpotentials and the Ohmic drop make efforts to reduce the bubble coverage attractive. Flowing electrolyte is often used to aid the early detachment of gas bubbles, before the bubbles covers a large surface area of the electrode, although this was found to make only a limited improvement.[21]

3.2.2 Total Bubble Volume

In the conventional set-up, while the bubble is migrating towards the top of the cell, it is directly between the two electrodes. The volume of solution displaced by the bubble will not be available for the transport of OH^- ions during this time, introducing a resistance to the direct transfer of OH^- ions from one electrode to the other.

At high current densities, there will be a large number of bubbles present, and the sum of the volumes of all the gas bubbles will become significant with regards to the total volume of the cell, and the volume of solution available for OH^- transport will be substantially reduced. This volume of bubbles is called the void fraction and an increase of the void fraction causes an increase in the electrical resistance of the solution.[5, 16, 22]

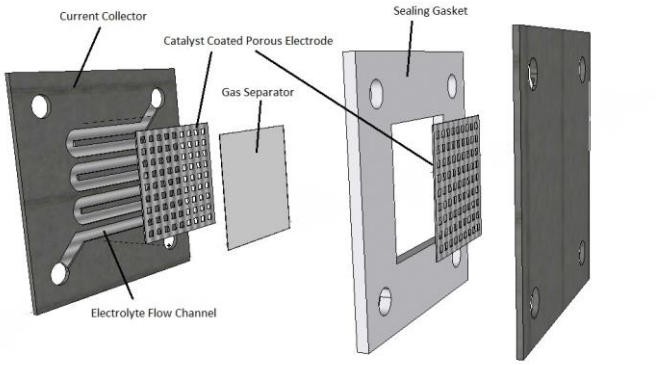

Figure 6 – A plot of cell voltage against the gap between electrodes at increasing current densities shows the existence of an optimal space between electrodes, becoming larger with increasing current densities. This shows the breakdown of Ohms law due to external influencing factors (Nagai *et al*.[18])

Nagai *et al.* demonstrated that when traditional electrolysers have high current densities and a small electrode gap, the void fraction becomes large and causes a significant increase in cell resistance, hence leading to a decrease in cell efficiency.[18] This can be seen in *figure 6* as the increase in cell voltage at electrode gaps below 2 mm, and current densities greater than 0.5 A·cm^{-2}.

The zero gap solution of using porous electrodes compressed onto the membrane, forces the gas bubbles to be released from the backside of the electrodes. The bubbles make a significantly smaller contribution to the void fraction, minimising the effect on the electrical resistance of the solution. This overcomes the optimal condition of 2 mm electrode spacing.

4. Zero Gap Cell Designs

4.1 Membrane Electrode Assembly

The central part of the zero gap design is called the Membrane Electrode Assembly (MEA) and includes the two porous electrodes in contact with either side of the membrane. There are different methods of producing the MEA which can be divided into two principal categories: Catalyst-Coated Substrate (CCS) and Catalyst-Coated Membrane (CCM).

Both methods employ porous electrodes, which offer the added benefit of increased active surface area, such that for the same material and cell design, a higher geometric current density can be achieved. The performance of the cell is dependent on the choice of catalysts and membranes as well as cell design, making comparisons between different cell designs difficult to quantify. Using Electrochemical Impedance Spectroscopy (EIS), the cell resistance R_{Cell} can be measured, and includes all interfacial contact resistances, resistance of the membrane and bubble effects in one value. When converted to the area resistance ($\Omega \cdot cm^2$), this value allows a degree of comparison between similar zero gap cells, and can help to guide the importance of cell design in overall cell performance. Where published, this value is reported.

In this section, the benefits and drawbacks of each type of assembly will be outlined, published examples introduced and the cell design bespoke to each system discussed.

4.2 Catalyst-Coated Substrates (CCS)

The CCS cell design involves a catalyst layer deposited directly onto a porous substrate, which is compressed onto either side of the membrane. The 'substrate' acts as both the electrode and the gas diffusion layer, and can take different forms. The original research into the zero gap setup was based around the catalyst coated substrate setup; using steel and nickel mesh electrode due to their wide availability and relatively low price.[12, 23] More recent research has involved a variety of different substrates and geometry, including porous carbon paper and porous nickel foam.[24, 25]

Mesh electrodes can be incorporated into a zero gap cell with a rugged and structurally sound design. The mesh is compressed either side of the membrane or gas separator using a bipolar plate with an integrated flow-field, to provide a path for electrolyte also to allow efficient removal of product gases from the cell. The flow of electrolyte can also remove heat from the cell when running at high current densities, which can be disposed of through a heat exchange in the external cell system. The setup is compressed together to ensure good connections and gaskets are used to prevent leaking, although care must be taken in this setup to avoid deformation of the membrane when applying compression.

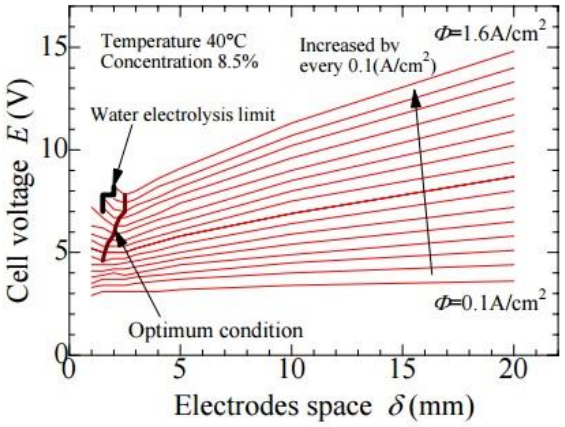

Figure 7 – 3D Schematic of a Catalyst Coated Substrate Zero Gap Cell, the two porous electrodes are individually coated with catalysts, and are pressed onto either side of the gas separator. The flow channels in the current collectors permit easily supply and removal of reactants/products.

Schiller *et al.* developed a high performing cell based around catalysed perforated nickel sheets, with circular electrodes of 600 cm^2 showing good performance and stability (300 $mA \cdot cm^{-2}$ at 1.65 V and 80 °C), even in intermittent conditions.[26]

Li et al. developed a 9 cm^2 test cell based on coated mesh, SS flow plates and an experimental alkaline anion exchange membrane from ITM Power, with current densities of 1 $A \cdot cm^{-2}$ at an initial voltage of 2.12 V, the cell showed stability during long term testing.[27]

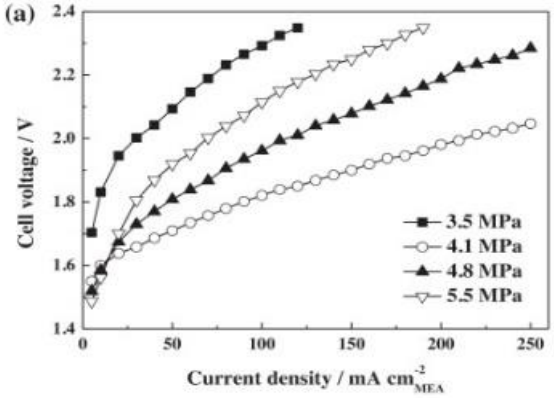

Figure 8 – A plot showing the effect of cell compression on overall cell performance – There exists an optimum compression where the electrical connection between the components is sufficient, but the components do not become deformed, in turn reducing the performance. (Ahn *et al.* [24]) This compression value is unique to each cell, but is an important parameter when optimising the cell performance.

Ahn *et al.* electrodeposited small amounts of Nickel directly onto carbon paper substrates and characterised a CCS test cell

using graphite bipolar plates. The cell compression pressure, *figure 8*, was seen to substantially affect cell performance, suggesting that the optimisation of this pressure is important when optimising the overall cell performance. The effect of this parameter was attributed to the contact resistance between the catalysed substrate and the graphite current collector flow plate.[24]

4.2.1 Nickel Foam

A variation of the CCS setup is achieved by using of high surface area electrodes such as Nickel foam, which has the advantage of a much higher active surface area than mesh substrates. The cell design is slightly altered as flow-field etched bipolar plates are no longer necessary, due to electrolyte flow through the porous material, although they are often still employed.

Gas management becomes an important factor due to the small pore size characteristic of the metal foam. When high current densities are applied, gas removal must be effective to stop the gas bubbles covering parts of the material, and reducing its available surface area. The large surface area provides a high number of sites for catalyst deposition, and one of the highest performing anodic electrodes reported is Ni/Fe $(OH)_2$ deposited onto a NF substrate.[28]

Xiao *et al.* used Ni-Fe catalysed Nickel foam and Ni-Mo catalysed stainless steel fibre felt hot pressed either side of an alkaline polymer electrolyte. The IR-free cell voltage for water electrolysis is expected to be about 1.7 V at 0.4 $A \cdot cm^{-2}$ and 40 °C.[29] It is noted that the IR loss cannot be neglected, and at a current density of 0.4 $A \cdot cm^{-2}$ and 70 °C the cell voltage is seen to be 1.85 V. The IR drop is attributed to the membrane-electrode contact, and the relatively thick cathode.

Seetharaman *et al.* developed a 6 cm^2 test cell with catalysed NF of thickness 0.22 mm, compressed between a titanium plate and the membrane. Teflon gaskets were used to prevent leakage, and the cell performance was reported as 1.9 V at 0.26 $A \cdot cm^{-2}$ for uncoated electrodes with a polystyrene based anion exchange membrane and 5.36 Molar KOH.[30] Activated electrodes produced 0.5 $A \cdot cm^{-2}$ for the same voltage. Electrolyte was flowed down the backside of the foam using a channelled titanium plate.

Kim *et al.* altered the nickel foam to fabricate an asymmetric porous nickel electrode, which had small pores (~5 µm) in contact with the membrane to provide the maximum active surface are, and a more open structure (pore size 100 µm) on the backside, to facilitate gas bubble removal from the bulk. Performance of 0.5 $A \cdot cm^{-2}$ was reported at a cell voltage of 1.8 V and 80 °C.[25] The gaskets were used as multifunctional sealants and electrolyte flow channels, such that the foam was compressed directly onto un-etched bipolar plate.

A research group at the Technical University of Denmark (DTU) have developed high temperature and pressure metal foam based alkaline electrolysis cells.[31] Charzichristodoulou *et al.* report a high temperature (250 °C) and pressure (40 bar) alkaline electrolysis cell with catalysed nickel foam based/metal alloy gas diffusion electrodes. The metal foams were compressed to a thickness of 0.5 mm, and were assembled either side of a novel electrolyte matrix tape. The high performance cell (3.75 $A \cdot cm^{-2}$ at 1.75 V) showed stability for 400 h, with a specific cell resistance of just 0.15 $\Omega \cdot cm^{-2}$.[32]

4.3 Catalyst Coated Membrane (CCM)

The CCM setup has been used in PEM electrolysis since its introduction, and is currently widely used in both PEM and Alkaline Fuel Cells. Benefits include lower catalyst loading, a thin catalytic layer and hydrophobicity. Recent work, particularly since the improvement of alkaline anion exchange membranes, has applied this setup to alkaline electrolysers with the aim of combining the benefits of PEM electrolysers with the less harsh alkaline environment.
This setup involves a catalytic layer consisting of catalyst nano-particles mixed with an ionomer/binder and dispersion solvent being deposited directly onto each side of the membrane. A gas diffusion layer is employed to provide an electrical connection from the catalyst layer to the bipolar plate, whilst also allowing the produced gas bubbles to escape; electrolyte is flowed through or behind the gas diffusion layer to facilitate gas removal. *Figure 9* shows an electrode printed directly onto a membrane.

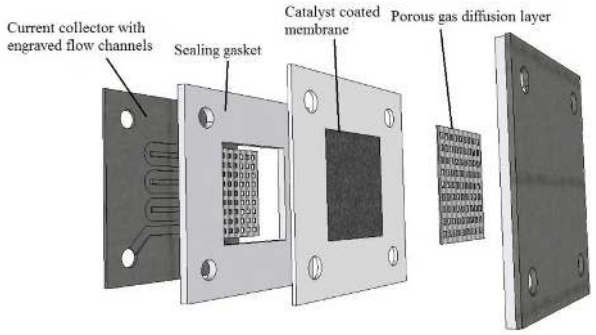

Figure 9 - Cell components for the catalyst coated membrane set-up. The catalyst is deposited directly onto the membrane, and the porous gas diffusion layers provide an electrical connection to the current collecting plate, whilst permitting the removal of produced gases.

Reported problems with the CCM method include the structural stability of the catalyst layers, with the possibility of the catalyst layers peeling off the membrane. The contact resistance between the gas diffusion layer and the catalyst layers has been investigated in similar PEMFC arrangements,[33] and it is reported to be an order of magnitude greater than that of the contact resistance between the gas diffusion layer and the bipolar plate, and even comparable to the resistance of the membrane.

Leng *et al.* prepared a CCM by hand spraying prepared catalyst ink onto either side of the membrane, the ink consisted of a catalyst (IrO_2 for anode, Pt for Cathode), de-ionized water, n-

propanol and AS-4 ionomer suspension. Titanium foam was used for the anodic gas diffusion layer and plain carbon paper for the cathodic gas diffusion layer, and they were mechanically pressed against the CCM when preparing the cell hardware. Initially the cell was fed with a pure water feed, 399 $mA \cdot cm^{-2}$ achieved at 1.8 V but better performance was observed with 1 Molar KOH.[34] With 1 Molar KOH, the cell resistance was 0.27 $\Omega \cdot cm^2$.

Wu *et al.* airbrushed catalyst inks onto either side of the membrane, and used stainless steel mesh as both gas diffusion layers and current collectors on each side. Using an alkaline anion exchange membrane, and a developed ionomer, the cell demonstrated 100 $mA \cdot cm^{-2}$ at 1.9 V.[13] Using electrochemical impedance spectroscopy, the electrolytic resistance was found to be 0.85 $\Omega \cdot cm^2$, and had a considerable effect on performance, especially towards 0.5 $A \cdot cm^{-2}$. Wu proposes that the use of the CCM method should reduce the ionic resistance between the catalyst layer and the membrane, since the catalyst layers should be hydrophobic and porous, the gas bubbles should be easily released and quickly replaced with water.

Pandiarajan and Ravichandran brush coated a spinel ferrite and Nickel powder on to the anodic and cathodic sides of a commercial AAEM, and used a pair of platinum coated titanium mesh as the current collectors. The cell exhibited a current density of 300 $mA \cdot cm^{-2}$ at 1.8 V in deionised water, with a lifetime of >100 hrs, the cell resistance was seen to be approx. 0.5 $\Omega \cdot cm^2$.[35]

4.3 Effect of Cell Design

The effects of zero gap cell design on cell performance can be broken down into three main areas: contact resistances, electrode geometry and mass transfer management.

Ahn *et al.* found that different compressions of the affected cell performance, which was the result of interfacial contact resistances between the different components of the cell. The zero gap cell needs to ensure good contact between the catalyst layer and the gas diffusion layer, and between the gas diffusion layer and the bipolar current collector. This area has attracted plenty of research for PEM electrolysers,[5] although limited research exists for zero gap alkaline electrolysers. The use of CCM's introduces an extra contact boundary, and the subsequent interfacial resistance. Future research should investigate this resistance to optimise the effecting parameters.
Choice of high surface area electrodes such as nickel foam can lead to a substantial scaling of current over other electrode substrates such as meshes,[10] although additional costs become an influencing factor.
Electrolyte flow is important to ensure the removal of product gases and the supply of electrolyte, particularly with foam electrodes. This will be important at high current densities when the amount of gas being produced is large.

Wu *et al.* calculated the electrolytic resistance of the cell, and showed the substantial increase in performance possible if this resistance could be substantially reduced.[13] *Figure 10* shows that when Ohmic resistance is isolated from other contributions to the cells overpotential, it is seen to be the prominent factor at high current densities. This emphasizes the necessary drive to reduce the contributions to the Ohmic resistance to achieve cells running at both high current densities and high efficiencies.

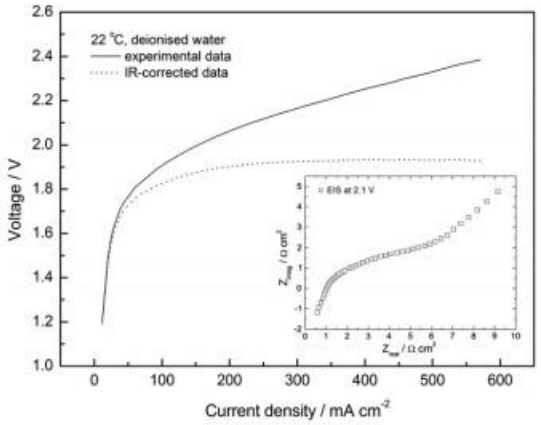

Figure 10 –A graph showing the cell voltage against current density with and without IR contributions. Eliminating the IR contributions shows a significant increase in performance, becoming more prominent at high current densities. (Wu *et al.*[13]) Research to reduce the IR contribution is crucial.

The aim of different cell designs is to provide high surface area of catalyst, low cell resistance and low material costs. The change from finite gap to zero gap setups significantly increases electrode surface area, and reduces R_{Cell} .

5. Materials for Zero Gap Alkaline Electrolysis

The zero gap design has 3 principal components: catalyst layer, gas diffusion layer and current collector. The alkaline environment permits the use of non-noble materials often based around Nickel due to its stability in basic conditions,[36] and to keep the cell costs well below that of PEM electrolysers, it is important these cheaper materials are utilized for these three components.

Catalysts used for traditional alkaline electrolysers have attracted a huge body of research,[37-40] and these materials can be directly applied to the zero gap setup. Pletcher *et al.* report that the current best catalysts as Ni-Mo for the cathode, and Ni-Fe $(OH)_2$ at the anode.[4, 27]

Gas diffusion layers based on Nickel Mesh/foam is used in many designs. Coated stainless steel is also a possibility on the cathodic side, although stainless steel experiences corrosion when subjected to high potentials in the presence of oxygen. Carbon cloth is employed in alkaline fuel cells although similarly due to oxidation at high potentials, it is not suitable for use on the anodic side.

Bipolar plates must provide good electrical conductivity, low contact resistance and corrosion resistance.[41] Titanium is

commonly used in PEM cells,[42] however plates based around stainless steel and nickel are attractive options for alkaline electrolysers due to low cost and are widely used. Graphite is used for bipolar plates in alkaline fuel cells however at the high potentials experienced on the anodic side make graphite unsuitable for this side of the alkaline electrolysis. Karimi *et al.* made a comparison of materials with regard to interfacial resistance for solid polymer fuel cells, stating that the increase in resistance over time is due to the formation of an insoluble oxide layer on the surface of the plate.[43]

6. Membranes

Large scale commercialisation of zero gap alkaline electrolysers is dependent on the development of membranes with excellent gas separation abilities coupled with a low resistance and long term stability in the alkaline environment. The next major advancement of advance alkaline electrolysers expected to be alkaline anion exchange membranes with performances closer to that of Nafion membranes used in the PEM environment. A full review of the current state of membrane development is worthy of a review in itself and, in fact, comparisons of developed membranes are available.[14]

Conclusions: Future Pathways for Research

The development of zero gap alkaline electrolysis to push its performance close to that of PEM electrolysis requires research in the three principal areas of catalysts, membranes, and cell design. The employment of the zero gap design demonstrates a substantially improved performance when compared to the traditional arrangement, and is allowing alkaline electrolysers to close the performance gap towards that of PEM electrolysers. It is crucial, however, that more development is undertaken to improve the cell design further. Each contribution to the cell resistance must be understood, particularly the interfacial contact resistances and the resistances contributed from bubble formation and removal, solutions must then implemented to reduce these contributions to the cell resistance. The use of high surface electrodes must be investigated to quantify their improvements in performance, and new geometries developed with further performance improvements.

7. References

1. T. S. Light, S. Licht, A. C. Bevilacqua and K. R. Morash, *Electrochemical and Solid-State Letters*, 2005, **8**, E16-E19.
2. K. Zeng and D. Zhang, *Progress in Energy and Combustion Science*, 2010, **36**, 307-326.
3. G. Passas and C. Dunnill, *J Fundam Renewable Energy Appl 5:* , 2015, -.
4. D. Pletcher and X. Li, *International Journal of Hydrogen Energy*, 2011, **36**, 15089-15104.
5. M. Carmo, D. L. Fritz, J. Mergel and D. Stolten, *International Journal of Hydrogen Energy*, 2013, **38**, 4901-4934.
6. M. A. Laguna-Bercero, *Journal of Power Sources*, 2012, **203**, 4-16.
7. J. Xu, G. Liu, J. Li and X. Wang, *Electrochimica Acta*, 2012, **59**, 105-112.
8. M. Schalenbach, G. Tjarks, M. Carmo, W. Lueke, M. Mueller and D. Stolten, *Journal of The Electrochemical Society*, 2016, **163**, F3197-F3208.
9. S. Marini, P. Salvi, P. Nelli, R. Pesenti, M. Villa, M. Berrettoni, G. Zangari and Y. Kiros, *Electrochimica Acta*, 2012, **82**, 384-391.
10. F. C. Walsh and D. Pletcher, in *Developments in Electrochemistry*, John Wiley & Sons, Ltd, Editon edn., 2014, pp. 95-111.
11. R. Costa and P. Grimes, *Chem. Eng. Prog.*, 1967, **63**, 56-58.
12. H. Wendt and H. Hofmann, *International Journal of Hydrogen Energy*, 1985, **10**, 375-381.
13. X. Wu and K. Scott, *Journal of Power Sources*, 2012, **214**, 124-129.
14. J. R. Varcoe, P. Atanassov, D. R. Dekel, A. M. Herring, M. A. Hickner, P. A. Kohl, A. R. Kucernak, W. E. Mustain, K. Nijmeijer, K. Scott, T. Xu and L. Zhuang, *Energy & Environmental Science*, 2014, **7**, 3135-3191.
15. M. S. U. F.Vogt, D. Burnat, A Zuttel, *8th International Symposium Hydrogen & Energy, Zhaoquing, China*, 2014.
16. R. L. LeRoy, M. B. I. Janjua, R. Renaud and U. Leuenberger, *Journal of The Electrochemical Society*, 1979, **126**, 1674-1682.
17. R. J. Gilliam, J. W. Graydon, D. W. Kirk and S. J. Thorpe, *International Journal of Hydrogen Energy*, 2007, **32**, 359-364.
18. N. Nagai, M. Takeuchi and T. Oka, *International Journal of Hydrogen Energy*, 2003.
19. H. Vogt, *Electrochimica Acta*, 2012, **78**, 183-187.
20. H. Vogt and R. J. Balzer, *Electrochimica Acta*, 2005, **50**, 2073-2079.
21. D. Zhang and K. Zeng, *Industrial & Engineering Chemistry Research*, 2012, **51**, 13825-13832.
22. G. Kreysa and M. Kuhn, *Journal of Applied Electrochemistry*, 1985, **15**, 517-526.
23. S. K. Mitra, P. Ragunathan and M. G. Nayar, *International Journal of Hydrogen Energy*, 1981, **6**, 497-507.
24. S. H. Ahn, B.-S. Lee, I. Choi, S. J. Yoo, H.-J. Kim, E. Cho, D. Henkensmeier, S. W. Nam, S.-K. Kim and J. H. Jang, *Applied Catalysis B: Environmental*, 2014, **154–155**, 197-205.
25. J.-H. Kim, J.-N. Lee, C.-Y. Yoo, K.-B. Lee and W.-M. Lee, *International Journal of Hydrogen Energy*, 2015, **40**, 10720-10725.
26. G. Schiller, R. Henne, P. Mohr and V. Peinecke, *International Journal of Hydrogen Energy*, 1998, **23**, 761-765.
27. X. Li, F. C. Walsh and D. Pletcher, *Physical Chemistry Chemical Physics*, 2011, **13**, 1162-1167.
28. X. Lu and C. Zhao, *Nat Commun*, 2015, **6**.

29. L. Xiao, S. Zhang, J. Pan, C. Yang, M. He, L. Zhuang and J. Lu, *Energy & Environmental Science*, 2012, **5**, 7869-7871.
30. S. Seetharaman, R. Balaji, K. Ramya, K. S. Dhathathreyan and M. Velan, *International Journal of Hydrogen Energy*, 2013, **38**, 14934-14942.
31. F. Allebrod, C. Chatzichristodoulou and M. B. Mogensen, *Journal of Power Sources*, 2013, **229**, 22-31.
32. C. Chatzichristodoulou, F. Allebrod and M. B. Mogensen, *Journal of The Electrochemical Society*, 2016, **163**, F3036-F3040.
33. I. Nitta, O. Himanen and M. Mikkola, *Electrochemistry Communications*, 2008, **10**, 47-51.
34. Y. Leng, G. Chen, A. J. Mendoza, T. B. Tighe, M. A. Hickner and C.-Y. Wang, *Journal of the American Chemical Society*, 2012, **134**, 9054-9057.
35. T. Pandiarajan, L. John Berchmans and S. Ravichandran, *RSC Advances*, 2015, **5**, 34100-34108.
36. D. E. Hall, *Journal of The Electrochemical Society*, 1981, **128**, 740-746.
37. W. Hu, *International Journal of Hydrogen Energy*, 2000, **25**, 111-118.
38. M. Bodner, A. Hofer and V. Hacker, *Wiley Interdisciplinary Reviews: Energy and Environment*, 2015, **4**, 365-381.
39. D. Pletcher, X. Li and S. Wang, *International Journal of Hydrogen Energy*, 2012, **37**, 7429-7435.
40. H. B. Suffredini, J. L. Cerne, F. C. Crnkovic, S. A. S. Machado and L. A. Avaca, *International Journal of Hydrogen Energy*, 2000, **25**, 415-423.
41. J. a. S. Richards, K *Alloy Steel - Properties and Use* 2011.
42. A. S. Gago, A. S. Ansar, P. Gazdzicki, N. Wagner, J. Arnold and K. A. Friedrich, *Meeting Abstracts*, 2014, **MA2014-02**, 1236.
43. S. Karimi, N. Fraser, B. Roberts and F. R. Foulkes, *Advances in Materials Science and Engineering*, 2012, **2012**, 22.